Final Report of the O3M-SAF Associated Scientist Activity

'Feasibility Study for Aerosol Retrieval over Land'

Otto Hasekamp
SRON, Netherlands Institute for Space Research
Sorbonnelaan 2
3584 CA Utrecht, The Netherlands

Corresponding author: email O.Hasekamp@sron.nl, tel. +31 30 253 8563, fax +31 30 254 0860

1 Overview

This final report summarizes the Associated Scientist activity on 'Feasibility Study for Aerosol Retrieval over Land', carried out during 3 months in the period January 2006-December 2006. This activity is a continuation of two earlier Associated Scientist activities carried out in 2003-2004 and 2005, respectively. The previous activities have resulted in the development of a prototype algorithm for aerosol retrieval over the ocean using the GOME-2 Polarization Measuring Device (PMD). During the current Associated Scientist activity we explored the possibilities for aerosol retrieval over land from GOME-2 measurements. For aerosol retrievals over land, the most important bottleneck is that the retrieved aerosol parameters are very sensitive to uncertainties in the surface reflection properties of the underlying surface. In this final report we will describe three possibilities to reduce the error on the retrieved aerosol properties due to errors in the surface reflection:

- Use only PMD measurements that show small sensitivity to surface reflection. Here, intensity measurements in the ultraviolet (336-384 nm) show small sensitivity to surface reflection because the albedo in the UV is generally low and the atmosphere is optically thick. So, the contribution of the surface to the total measured intensity in the UV is small. Furthermore, the albedo is spectrally flat in this spectral range which allows to retrieve one surface albedo for the UV spectral range. The measurements of Stokes parameter Q show small sensitivity to surface reflection over the whole spectral range thus all measurements of Q can be used. This option was investigated and it was found that due to the fact intensity measurements in the range 400-800 nm were omitted, the information on aerosol properties decreased significantly, i.e. the results become strongly dependent on *a priori* information on aerosol microphysical properties. This leads to regularization errors on the optical thickness in the range 0.15-0.25, and retrieval errors of about 0.05.

- Use PMD measurements in the full spectral range (336-792 nm) and fit coefficients of a number of standard albedo spectra simultaneously with the aerosol properties. Here, we considered the retrieval of 5 standard albedo spectra. We found that due to overlap of spectral feature of the albedo spectra with spectral features of aerosol properties, the results become dependent on *a priori* information on the albedo spectra and aerosol properties. This leads to regularization errors on the optical thickness in the range 0.1-0.2, similar to the previous option. The retrieval noise is about 0.02, which is less than for the previous option.

- Use measurements of Stokes parameter Q over the full spectral range combined with intensity measurements in the range 336-384 nm and additionally intensity measurements in the 3 absorption bands of Oxygen in the GOME-2 spectral range. Here, due to the characteristic spectral signature of Oxygen, the surface contribution can be separated from the atmospheric contribution. This approach results in regularization and retrieval errors of about 0.05 on the aerosol optical thickness. This is significantly better than the other 2 options. However, a possible drawback of this option is that retrievals have to be performed at the spatial resolution of the GOME-2 main channels, which is much worse than that of the PMD.

We will describe the three options in more detail in this final report.

2 Background

Aerosols directly affect the Earth's climate by scattering and absorption of radiation, and indirectly by changing the micro-physical properties of clouds. The total effect of aerosols on climate is very uncertain, both in magnitude and even in sign, representing one of the largest uncertainties in climate research. In order to improve our understanding of the effect of aerosols on climate, global measurements are needed of a number of aerosol properties such as aerosol size, refractive index and optical thickness. The only way to obtain these measurements at a global scale is by means of satellite remote sensing.

Many satellite instruments that are used for aerosol retrieval are multiple-wavelength single-viewing-angle instruments. Among these instruments are the Advanced Very High Resolution Radiometer (AVHRR), the Moderate Resolution Imaging Spectroradiometer (MODIS), the Total Ozone Mapping Spectrometer (TOMS), the Global Ozone Monitoring Experiment (GOME) and the Scanning Imaging Absorption Spectrometer for Atmospheric Chartography (SCIAMACHY). Although it has been shown that the aerosol optical thickness may be retrieved from these instruments [*Mishchenko et al.*, 1999; *Tanré et al.*, 1999; *Veefkind et al.*, 2000; *Torricella et al.*, 1999], the results depend critically on the assumed values of the other aerosol parameters (size distribution, refractive index). The aerosol information content of intensity measurements is significantly larger for instruments that perform measurements at multiple viewing angles, such as the Multiangle Imaging Spectro-Radiometer (MISR), and the Advanced Along-Track Scanning Radiometer (AATSR). However, the combined use of intensity and polarization measurements at multiple viewing angles have been shown to be most powerful for the purpose of aerosol retrieval [*Mishchenko and Travis*, 1997a, b; *Chowdhary et al.*, 2001]. The reason for this is the high sensitivity of polarization properties of light to aerosol micro-physics [*Hansen and Travis*, 1974]. Satellite measurements of intensity and polarization at 14 viewing angles in the spectral range 443-865 nm have been performed by the Polarization and Directionality of Earth's Reflectances-1 and -2 instruments (POLDER-1 and -2). Both instruments were active for about 8 months in 1996/1997 and 2002, respectively. Since the end of 2004 the PARASOL instrument, which is a somewhat adjusted version of POLDER, is flying on the CALYPSO satellite. Aerosol retrievals from POLDER have been reported, among others, by *Deuzé et al.* [2000, 2001] and *Herman et al.* [2005]. The Aerosol Polarimetric Sensor (APS) [*Travis*, 1993] is a future planned instrument that will perform multiple-viewing-angle measurements of intensity and polarization in a broader spectral range (410-2250 nm) than POLDER and at more viewing angles (152 angles). Chowdhary and co-workers [*Chowdhary et al.*, 2001, 2002, 2005] have demonstrated the potential of APS for the retrieval of aerosol properties using the Research Scanning Polarimeter (RSP), which is functionally similar to APS.

The Global Ozone Monitoring Experiment-2 (GOME-2) is a single-viewing angle instrument that measures the backscattered intensity in the spectral range 240-800 nm at a spectral resolution of 0.2-0.4 nm. The spatial resolution of these measurements is expected to be 40×40 km^2. GOME-2 also contains a polarization measuring device (PMD) that measures the Stokes parameters I and

Table 1: Probable PMD band selection for GOME-2 [*Hasekamp et al.*, 2004]. The wavelength range is indicated by the center wavelengths of the first and last PMD pixel, respectively, not including the Full Width at Half Maximum (FWHM) of the slit function, which is shown in the last column.

Band nr.	Wavelength range(nm)	Nr. of pixels	FWHM(nm)
1	spare	-	-
2	311.8-314.3	5	3.1
3	316.9-318.8	4	3.3
4	321.5-329.3	12	3.5
5	330.8-334.6	6	3.8
6	336.2-340.0	24	4.8
7	361.0-377.9	20	4.8
8	380.3-383.9	4	6.1
9	399.8-428.0	19	7.8
10	435.1-493.5	23	10.2
11	495.5-552.4	23	12.5
12	567.9-598.0	5	25.2
13	600.0-660.0	11	30.0
14	743.1-766.6	3	38.5
15	783.6-792.4	2	43.9

Q in 15 spectral bands (see Table 1) in the range 300-800 nm, at a much better spatial resolution than the main channels of 5×40 km^2. The GOME-2 polarization measurements are significantly improved compared to those of GOME and SCIAMACHY, both in spectral sampling and accuracy. As demonstrated by *Hasekamp and Landgraf* [2005b], the polarization measurements of GOME-2 provides an interesting option for the purpose of aerosol retrieval. During previous O3M-SAF Associated Scientist activities an approach was developed for aerosol retrieval over the ocean that makes full use of the capabilities of GOME-2. In this retrieval approach all parameters describing a bimodal aerosol model are considered as unknown parameters. This results in the following 8 unknown aerosol parameters to be retrieved: the effective radius r_{eff} of both modes, the effective variance v_{eff} of both modes, the aerosol column N of both modes, and the real and imaginary part of the refractive index $m = m_r + im_i$. Additionally, the height of the layer where the bulk of the aerosol is located and the oceanic pigment concentration are included as unknown parameters. The parameters are retrieved using a linearized radiative transfer model combined with Phillips-Tikhonov regularization [*Hasekamp and Landgraf*, 2005a, b].

The retrieval of aerosol properties is known to be very sensitive to uncertainties in the reflection properties of the Earth surface. Therefore, the previous Associated Scientist activities were restricted to retrievals over the ocean, where surface reflection properties are known relatively well. Here the diffuse ocean albedo depends on the oceanic pigment concentration that can be retrieved simultaneously with the aerosol parameters. The situation is more complex for aerosol retrievals over land, where the spectral surface albedo cannot be described by a single parameter. Most retrieval schemes use *a priori* information from a satellite based surface albedo climatology [*Torres et al.*, 2001]. However, uncertainties in the used surface albedos represent one of the largest error sources on retrieved aerosol properties. In this study three different approaches are investigated to reduce the error on the retrieved aerosol properties due to errors in the surface reflection: (1) The use of measurements that have only small sensitivity to surface reflection (Stokes parameter Q and intensity measurements in the UV in the range 336-384 nm), (2) The simultaneous retrieval of aerosol properties and a number of standard albedo spectra, and (3) the use of polarization measurements (Stokes parameter Q), intensity measurements in the range 336-384 nm, and intensity measurements in the Oxygen absorption bands, where the characteristic spectral dependence of Oxygen absorption allows one to separate the atmospheric contribution from the surface contribution.

3 Retrieval Approach

3.1 Aerosol Properties

In this paper we assume that the aerosol size distribution can be described by a bi-modal log normal function. Here, each mode is characterized by the effective radius r_{eff}, the effective variance v_{eff} (see e.g. *Hansen and Travis* [1974]) and the aerosol loading N. In what follows we use the superscripts l and s to refer to the small- and large mode of the size distribution, respectively. Additionally, the complex refractive index $m = m_r + im_i$ is needed to characterize aerosols. Furthermore, we assume an altitude distribution with a constant aerosol density ρ_o in the lowest layer with height z_b of the atmosphere. Above that layer the aerosol density decreases with the 4-th power in pressure p till a certain height z_t above which we assume no aerosols are located, i.e.

$$\begin{aligned} \rho(z) &= \rho_o && \text{for } z < z_b \\ \rho(z) &= \rho_o(p(z)/p(z_b))^4 && \text{for } z_b < z < z_t \\ \rho(z) &= 0 && \text{for } z > z_t. \end{aligned} \qquad (1)$$

In our retrievals we consider 9 unknown aerosol parameters. These are the effective radius r_{eff} of the small- and large mode, the effective variance v_{eff} of the small- and large mode, the aerosol loading N of the small- and large mode, the real- and imaginary part of the refractive index, and the height z_b of the layer where the bulk of the aerosols is located. Here,we assume that the wavelength dependence of the refractive index is known.

3.2 Forward model and Inversion

Let us define a state vector $\mathbf{x}$ that contains the parameters to be retrieved. Furthermore, let us define a measurement vector $\mathbf{y}$ that contains the satellite measurements of Stokes parameters I and Q in different spectral bands. The retrieval of state vector $\mathbf{x}$ from measurement vector $\mathbf{y}$ requires a forward model $\mathbf{F}$ that describes how $\mathbf{y}$ and $\mathbf{x}$ are related, viz.

$$\mathbf{y} = \mathbf{F}(\mathbf{x}) + \mathbf{e}_y, \qquad (2)$$

where $\mathbf{e}_y$ is an error term. The forward model consists of two parts. The first part relates the physical aerosol properties (size distribution, refractive index) to their optical properties (optical thickness, single scattering albedo, phase matrix). This relation can be described by Mie theory for spherical particles [*van de Hulst*, 1957] or alternative theories for particles with other shapes (see e.g. *Kokhanovsky* [2003]; *Wiscombe and Grams* [1988]; *Koepke and Hess* [1988]; *Mishchenko and Travis* [1994]; *Mishchenko et al.* [1995]). In this paper we only consider spherical aerosols which allows the use of Mie theory. The second part of the forward model is an atmospheric radiative transfer model that simulates the intensity vector at the top of the atmosphere for given optical input parameters. Here, we use the vector radiative transfer model described by *Hasekamp and Landgraf* [2002] and *Hasekamp and Landgraf* [2005a], to model the transport of radiation in the atmosphere This model solves the radiative transfer equation using the Gauss-Seidel iterative method.

The aim of an inversion algorithm is to find a state vector $\hat{\mathbf{x}}$ for which forward model $\mathbf{F}(\hat{\mathbf{x}})$ and measurement $\mathbf{y}$ are in optimal agreement. Since the forward model is not linear in the unknown parameters the solution of the inversion problem has to be found iteratively. Here, we replace for each iteration step n the forward model in (2) by its linear approximation,

$$\mathbf{F}(\mathbf{x}_{n+1}) \approx \mathbf{F}(\mathbf{x}_{\mathrm{n}}) + \mathbf{K}\left[\mathbf{x}_{\mathrm{n+1}} - \mathbf{x}_{\mathrm{n}}\right] \tag{3}$$

where $\mathbf{x}_{\mathrm{n}}$ is the state vector for the iteration step under consideration and $\mathbf{K}$ is the Jacobian matrix containing the derivatives of the forward model with respect to the elements of $\mathbf{x}_n$, where element K_{ij} of $\mathbf{K}$ is defined by:

$$K_{ij} = \frac{\partial F_i}{\partial x_j}(\mathbf{x}_{\mathrm{n}}). \tag{4}$$

The satellite measurements considered here do not contain sufficient information to retrieve all 10 unknown parameters, and thus the corresponding inverse problem is ill-posed. This means that many combinations of the 10 parameters fit the measurement almost equally well. As a result, the least-squares solution $\hat{\mathbf{x}}_{\mathrm{lsq}}$ to our retrieval problem, viz.

$$\hat{\mathbf{x}}_{\mathrm{lsq}} = \min_{\mathbf{x}} ||\mathbf{S}_y^{-\frac{1}{2}}(\mathbf{F}(\mathbf{x}) - \mathbf{y})||^2, \tag{5}$$

is overwhelmed by noise. In order to reduce the effect of noise, we use the Phillips-Tikhonov regularization method [*Phillips*, 1962; *Tikhonov*, 1963], which introduces a side constraint in addition to the minimization of the least-squares norm. As a side constraint we choose for our application the minimization of a weighted norm of the state vector, viz.

$$\hat{\mathbf{x}}_{\mathrm{reg}} = \min_{\mathbf{x}} \left(||\mathbf{S}_y^{-\frac{1}{2}}(\mathbf{F}(\mathbf{x}) - \mathbf{y})||^2 + \gamma\, ||\mathbf{\Gamma}\mathbf{x}||^2 \right), \tag{6}$$

where $\mathbf{\Gamma}$ is a diagonal matrix that contains weighting factors for the different state vector elements in the side constraint, and the regularization parameter γ balances the two minimizations in (6). For each iteration step the solution $\hat{\mathbf{x}}_{\mathrm{reg,n+1}}$ in (6) can be written as a matrix equation:

$$\hat{\mathbf{x}}_{\mathrm{reg,n+1}} = \mathbf{D}\,\tilde{\mathbf{y}} \tag{7}$$

where $\tilde{\mathbf{y}} = \mathbf{y} - \mathbf{F}(\mathbf{x}_\mathrm{n}) + \mathbf{K}\mathbf{x}_\mathrm{n}$, and $\mathbf{D}$ is the contribution matrix defined by

$$\mathbf{D} = \left(\mathbf{K}^T\, \mathbf{S}_y^{-1}\, \mathbf{K} + \gamma\mathbf{\Gamma}\right)^{-1}\; \mathbf{K}^T\, \mathbf{S}_y^{-1}, \tag{8}$$

where the superscript T denotes the transposed matrix.

The rationale of minimizing the norm of the state vector as a side constraint in (6) is to reduce the effect of measurement noise on the solution. Since the norm of the state vector is a quantity that is very sensitive to noise contributions, these contributions are reduced using (6) instead of (5). Clearly, a good choice of γ is of crucial importance for the Phillips-Tikhonov solution. If γ is chosen too large, the noise contribution will be low but the least squares norm deviates significantly from its minimum value, i.e. the fit between forward model and measurement is poor. On the other hand, if γ is chosen too small the measurement is fitted well but the solution norm is high, i.e. the solution is overwhelmed by noise. Thus, γ should be chosen such that the two minimizations are well balanced. Such a value for γ can be found from the L-curve [*Hansen and O'Leary*, 1993]. The L-curve is a parametric plot of the weighted least squares norm $||\mathbf{S}_y^{-\frac{1}{2}}(\mathbf{F}(\mathbf{x})-\mathbf{y})||$ and the weighted solution norm $||\mathbf{\Gamma}\mathbf{x}||$, with a characteristic L-shaped corner. The corner of the L-curve corresponds to the optimum value of the regularization parameter. A numerical stable and efficient method for determining the corner of the L-curve is given by *Hansen* [1992]. They define the corner of the L-curve as the point with maximum curvature, where the curvature is calculated analytically. Visual inspection of the L-curves of our retrievals showed that in all cases the method of *Hansen* [1992] provided a value for the regularization parameter that corresponds to the 'true' corner of the L-curve.

Due to the inclusion of the side constraint, the state vector $\hat{\mathbf{x}}_\mathrm{reg}$ retrieved using (6) does not represent an estimate of the true state vector $\mathbf{x}_\mathrm{true}$, but its elements represent weighted averages of the elements of $\mathbf{x}_\mathrm{true}$. The relation between $\hat{\mathbf{x}}_\mathrm{reg}$ and $\mathbf{x}_\mathrm{true}$ is expressed by the averaging kernel $\mathbf{A}$ [*Rodgers*, 2000], viz.

$$\hat{\mathbf{x}}_\mathrm{reg} = \mathbf{A}\mathbf{x}_\mathrm{true} + \mathbf{e}_x. \tag{9}$$

Here, $\mathbf{e}_x$ represents the error in the state vector caused by measurement errors, and the averaging kernel is given by

$$\mathbf{A} = \frac{\partial \hat{\mathbf{x}}}{\partial \mathbf{x}_\mathrm{true}} = \frac{\partial \hat{\mathbf{x}}}{\partial \mathbf{x}_\mathrm{true}} = \left(\mathbf{K}^T\, \mathbf{S}_y^{-1}\, \mathbf{K} + \gamma\mathbf{\Gamma}\right)^{-1}\; \mathbf{K}^T\, \mathbf{S}_y^{-1}\, \mathbf{K} = \mathbf{D}\,\mathbf{K}. \tag{10}$$

The matrix $\mathbf{A}$ is strongly related with the information content of the measurement $\mathbf{y}$, i.e. the closer $\mathbf{A}$ is to the unity matrix, the higher the information content. From the matrix $\mathbf{A}$ the Degrees of Freedom for Signal (DFS) can be derived [*Rodgers*, 2000], which indicates the number of independent pieces of information that is retrieved from the measurement:

$$\mathrm{DFS} = \mathrm{trace}\,(\mathbf{A}). \tag{11}$$

If $\mathbf{x}_\mathrm{true}$ would have represented a discretization of a continuous function, then the weighted averages contained in $\hat{\mathbf{x}}_\mathrm{reg}$ (9) would have a clear physical meaning, i.e. an estimate of $\mathbf{x}_\mathrm{true}$ at a reduced resolution. However, for our application the elements of $\hat{\mathbf{x}}_\mathrm{reg}$ represent weighted averages of different aerosol parameters, which have a limited physical meaning. Therefore, we include information from an *a priori* state vector $\mathbf{x}_a$ in the solution to make it a meaningful estimate of the $\mathbf{x}_{\text{true}}$. Hereto, we add the term $(\mathbf{I}-\mathbf{A})\mathbf{x}_a$ to $\hat{\mathbf{x}}_{\text{reg}}$ in order to obtain the final retrieval product $\hat{\mathbf{x}}$, viz.

$$\begin{aligned}\hat{\mathbf{x}} &= \hat{\mathbf{x}}_{\text{reg}} + (\mathbf{I}-\mathbf{A})\mathbf{x}_a, \\ &= \mathbf{A}\mathbf{x}_{\text{true}} + (\mathbf{I}-\mathbf{A})\mathbf{x}_a + \mathbf{e}_x. \end{aligned} \tag{12}$$

Thus, in (12) $\hat{\mathbf{x}}_{\text{reg}}$ represents an estimate of $\mathbf{A}\mathbf{x}_{\text{true}}$ and $(\mathbf{I}-\mathbf{A})\mathbf{x}_a$ represents an estimate of the part $(\mathbf{I}-\mathbf{A})\mathbf{x}_{\text{true}}$ of the true state vector that cannot be retrieved from the measurement. Here, the dependence of a retrieved element $\hat{x}_i$ of the state vector on its corresponding *a priori* value $x_{a,i}$ is given by

$$\frac{\partial \hat{x}_i}{\partial x_{a,i}} = 1 - a_{ii}, \tag{13}$$

where a_{ii} is element (i,i) of $\mathbf{A}$. An equation similar to to (12) has been used by *Rodgers and Connor* [2003] to represent retrieval results with respect to a different *a priori* state vector than had been used in the retrieval. The reason that we first solve the minimization problem (6) and later add *a priori* information in (12), instead of directly including $\mathbf{x}_a$ in the side constraint of (6), is that in our approach the amount of information extracted from the measurement is independent from the *a priori* state vector $\mathbf{x}_a$. So, this approach is especially suited for characterizing the information content of satellite measurements, which is an important aspect of this paper.

The weighting factors in the matrix $\mathbf{\Gamma}$ are defined relative to the values of the corresponding state vector element for the iteration step under consideration. This makes the vector $\mathbf{\Gamma x}$ dimensionless. From (6) it can be seen that if the weighting factor for a certain parameter decreases while the other weighting factors are kept constant, more information about this parameter is obtained from the measurement. This means that the parameters with small relative weight are less dependent on the *a priori* information added in (12). So, if for certain state vector elements less reliable *a priori* information is available than for others, the relative weighting factors corresponding to these parameters should be set to small values. In this way the dependence on *a priori* for the state vector elements with small relative weight becomes smaller while for the other parameters the dependence on *a priori* becomes larger, compared to the situation where all parameters have unity relative weight. For our application it may be expected that no reliable *a priori* information will be available for the aerosol columns of both modes, because these two parameters are highly variable. Therefore, the relative weighting factors corresponding to these two parameters are set to a very low value ϵ while the other factors get a unity relative weight. We found that for $\epsilon = 1 \times 10^{-8}$ the retrieved aerosol columns for both modes are virtually independent from their *a priori* values.

From (12) it is clear that the retrieved state vector $\hat{\mathbf{x}}$ is affected by errors in the *a priori* state vector $\mathbf{x}_a$. The error on $\hat{\mathbf{x}}$ caused by an error on $\mathbf{x}_a$ is called the regularization error (called smoothing error by [*Rodgers*, 2000]). The regularization error covariance matrix $\mathbf{S}_r$ is given by

$$\mathbf{S}_r = (\mathbf{I}-\mathbf{A})\, \mathbf{S}_a\, (\mathbf{I}-\mathbf{A})^T, \tag{14}$$

where $\mathbf{S}_a$ is the *a priori* covariance matrix. Ideally, $\mathbf{S}_a$ is calculated from an ensemble of states that also include the retrieved state [*Rodgers and Connor*, 2003]. However, for the application of aerosol satellite remote sensing $\mathbf{S}_a$ is in general not known which makes it difficult to calculate $\mathbf{S}_r$ for individual retrievals. However, an estimate for the upper boundary of the regularization error can be obtained by calculating $\mathbf{S}_r$ from (14) by assuming an *a priori* covariance matrix representing maximum values for the errors on the elements of $\mathbf{x}_a$. In order to estimate the maximum errors on the elements of $\mathbf{x}_a$ we used the 17 tropospheric aerosol models of *Torres et al.* [2001]. For these 17 aerosol models we calculated the mean value and considered the maximum difference between the mean value and the actual value as *a priori* error. This resulted in the following values σ_a for the *a priori* error: $\sigma_a(r^s_{\text{eff}}) = 0.05\ \mu$m, $\sigma_a(v^s_{\text{eff}}) = 0.23, \sigma_a(r^l_{\text{eff}}) = 1.29\ \mu$m, $\sigma_a(v^l_{\text{eff}}) = 0.22, \sigma_a(m_r) = 0.065$, and $\sigma_a(m_i) = 0.01$. For z_b we assumed *a priori* errors of 100 %.

The contribution matrix $\mathbf{D}$ plays an important role for calculating the error propagation from measurement $\mathbf{y}$ to state vector $\mathbf{x}$. The effect of a random measurement error on the state vector is called retrieval noise. The retrieval noise covariance matrix $\mathbf{S}_x$ is given by

$$\mathbf{S}_x = \mathbf{D}\ \mathbf{S}_y\ \mathbf{D}^T \tag{15}$$

Systematic state vector errors $\Delta\mathbf{x}$ due to systematic measurement errors $\Delta\mathbf{y}$ can also be evaluated using the contribution matrix:

$$\Delta\mathbf{x} = \mathbf{D}\ \Delta\mathbf{y} \tag{16}$$

and a similar expression holds for systematic forward model errors $\Delta\mathbf{F}$, but with $\Delta\mathbf{y}$ replaced by $-\Delta\mathbf{F}$. Of course, the systematic errors in measurement and forward model are not known, because otherwise they would have been corrected for. However, examples of systematic state vector errors can be calculated for some reasonable scenarios of systematic measurement- and forward model errors.

For estimating direct radiative forcing by aerosols, aerosol optical properties such as (spectral) optical thickness and single scattering albedo are very important. These optical properties can be derived from the micro-physical aerosol parameters contained in the state vector $\mathbf{x}$. The standard deviation σ_τ on the optical thickness can be obtained from the retrieval noise covariance matrix $\mathbf{S}_x$ via

$$\sigma_\tau = \sqrt{\sum_{i=1}^{N}\sum_{j=1}^{N}\ s_{i,j}\ \frac{\partial\tau}{\partial x_i}\ \frac{\partial\tau}{\partial x_j}} \tag{17}$$

where $s_{i,j}$ denotes element (i,j) of $\mathbf{S}_x$. The effect of the regularization error covariance matrix can be obtained in the same way. Systematic errors $\Delta\tau$ on the aerosol optical thickness τ are given by

$$\Delta\tau = \sum_{i=1}^{N}\Delta x_i\ \frac{\partial\tau}{\partial x_i}. \tag{18}$$

Expressions similar to (17) and (18) hold for the aerosol single scattering albedo ω.

From (11), (14), (15), and (16) it follows that in order to perform a retrieval of aerosol properties and to characterize its information content and sensitivity to different types of errors, we need in addition to measurement information, the contribution matrix (8) and the averaging kernel (10). To calculate these matrices the Jacobian matrix $\mathbf{K}$ (4) is needed. This means that a vector radiative transfer model is needed that calculates the Jacobian matrix $\mathbf{K}$, i.e. the derivatives of the

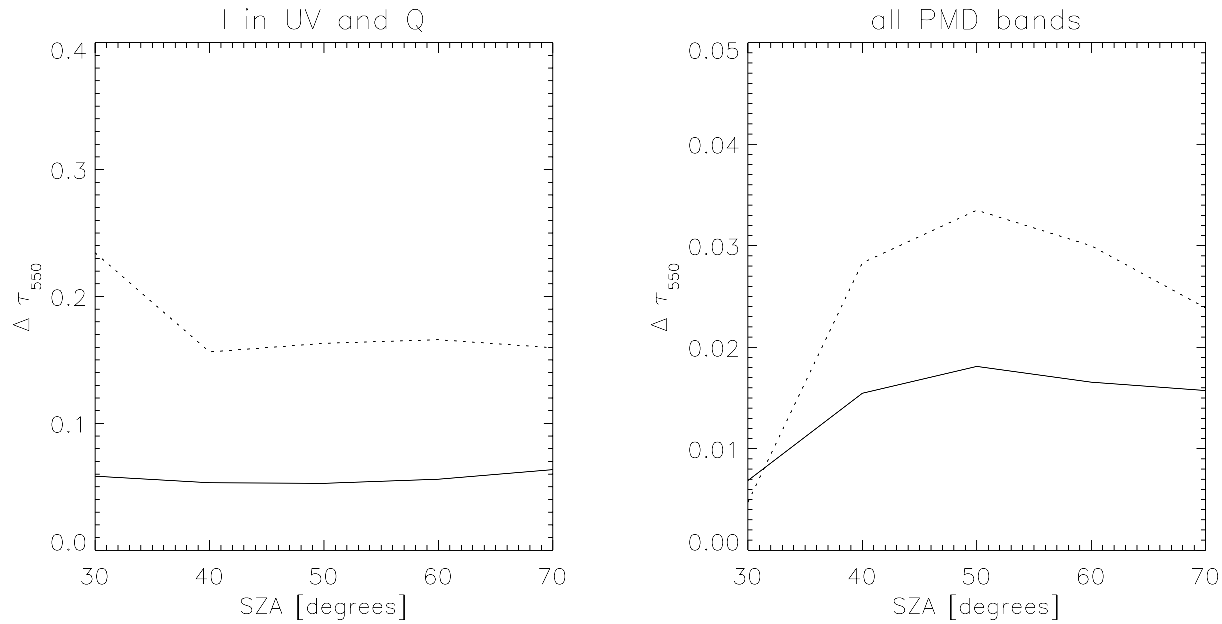

Figure 1: (left panel) Retrieval error (solid line) and regularization error (dotted line) for retrievals using measurements of I in PMD bands 6-8 and measurements of Q in PMD bands 6-15. A constant albedo for the UV range is fitted together with the aerosol properties. (right panel) Retrieval error (solid line) and regularization error (dotted line) for retrievals using measurements of I and Q in PMD bands 6-15.

Stokes parameters with respect to the parameters to be retrieved, in addition to the measurement simulation. For the calculations in this paper we use the vector radiative transfer model described by *Hasekamp and Landgraf* [2005a], which calculates these derivatives in an analytical way. The validity of linear error mapping, as used in (15) and (16), for the application of aerosol retrieval has been demonstrated by *Hasekamp and Landgraf* [2005a].

4 Possibilities for Aerosol Retrieval over Land

4.1 Reduced Spectral Range for Intensity

In order to reduce the error on the retrieved aerosol properties due to uncertainties in surface albedo, it is an option to only consider measurements of the GOME-2 PMD that have a low sensitivity to surface reflection. In this study, we use for this purpose intensity measurements at wavelengths < 384 nm and measurements of Stokes parameter Q over the full spectral range. Leaving out the PMD measurements that interfere with ozone absorption, this means that intensity measurements from PMD 6-8 can be used and measurements of Stokes parameter Q from PMD 6-15 (see Table 1). We performed aerosol retrievals on a measurement vector that contained these measurements, where we considered one constant surface albedo in the UV as an unknown parameter, in addition to the aerosol parameters.

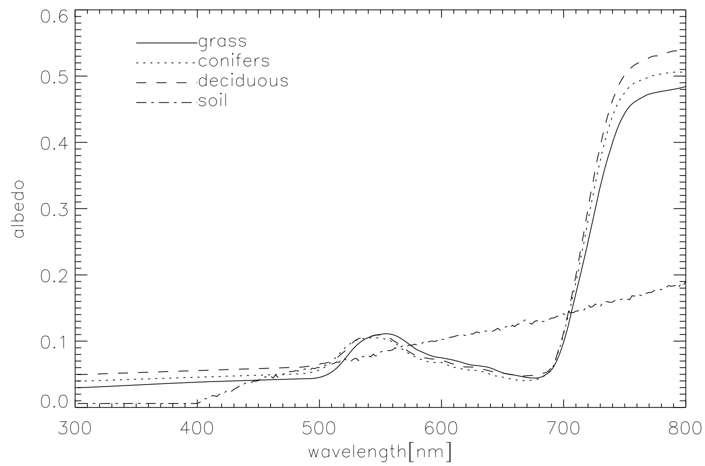

Figure 2: Surface albedo spectra used in this study. The surface albedo spectra are reproduced from the ASTER Spectral Library through the courtesy of the Jet Propulsion Laboratory, California Institute of Technology, Pasadena, California. Copyright 1999, California Institute of Technology. ALL RIGHTS RESERVED.

Figure 1 (left panel) shows the error on the optical thickness at 550 nm, as a function of solar zenith angle (SZA) for these retrievals. For comparison, also the optical thickness error for retrievals using PMD measurements in bands 6-15 for both I and Q is shown in the right panel of Fig. 1. As described in the previous section, the retrieval error in Fig. 1 indicates the effect of measurement errors on the retrieved optical thickness, whereas the regularization error indicates the effect of *a priori* assumptions about aerosol microphysical properties on the retrieved optical thickness.

It follows from Fig. 1 that when measurements of I in band 9-15 are left out of the measurement vector, both the retrieval error and regularization error increase significantly. Here, the retrieval error increases from about 0.015 to 0.06, whereas the regularization error increases from 0.02-0.03 to 0.15-0.20. The large regularization error means that the aerosol retrievals that leave out PMD intensity measurements in band 9-15 become very sensitive to *a priori* information on aerosol microphysical properties. The reason for this is that due to the reduced spectral range for measurements of I, less information on aerosol microphysical properties can be retrieved from the measurements, namely the Degrees of Freedom for Signal decreases from 7 to 5 when measurements of I in band 9-15 are left out. The missing pieces of information have to be assumed *a priori*, which causes the large regularization errors on the optical thickness. So, the use of a limited spectral range for intensity measurements in order to reduce the sensitivity to surface albedo, is only a useful option if accurate information on aerosol microphysical properties is available, for example from AERONET [*Dubovik et al.*, 2002] measurements.

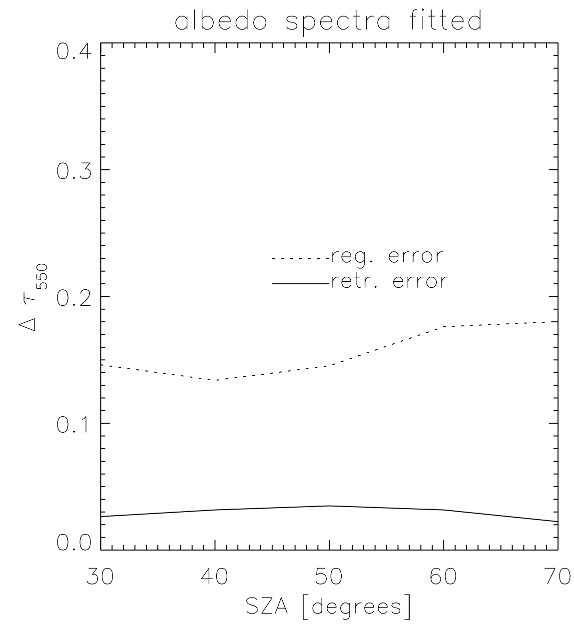

Figure 3: Retrieval error (solid line) and regularization error (dotted line) for retrievals using measurements of I and Q in PMD bands 6-15, where coefficients for the albedo spectra of Fig. 2 were retrieved together with the aerosol parameters. We assumed an *a priori* error of 20 % in the coefficients.

4.2 Retrieval of Standard Albedo Spectra

Another possibility for aerosol retrieval over land is to fit coefficients for a number of standard albedo spectra together with the aerosol properties, and use the full spectral range 336-792 nm for measurements of both I and Q (PMD bands 6-15). We investigated this option using the 4 albedo spectra depicted in Fig. 2, which describe the reflection properties of grass, conifers, deciduous, and soil, respectively. In addition to these 4 albedo spectra we included a constant albedo in the retrieval to compensate for an offset in the albedo spectra.

Figure 3 shows the retrieval error and regularization error on the optical thickness at 550 nm for the corresponding retrievals. It can be seen that compared to Fig. 1, where the spectral range of the intensity was restricted to 336-384 nm, the retrieval error in Fig. 3 is about a factor 2 smaller while the regularization error is similar to that shown in Fig. 1. So, also when a larger spectral range for intensity measurements is used and albedo spectra are fitted together with the aerosol properties the regularization error is large. This is due to the fact that there is spectral overlap between the effect of aerosol properties on the measurement and the effect of the albedo spectra (especially the soil spectrum and the offset). This results in a large contribution of *a priori* information on aerosol properties in the solution, which leads to the large regularization errors in Fig. 3. Although the retrieval error is somewhat smaller in Fig. 3 compared to Fig. 1, we do not consider it a better option to fit standard albedo spectra together and use the full spectral range for I and Q (Fig. 3) than to limit the spectral range for the intensity measurements (Fig. 1). Namely, for retrievals on real measurements it is probably necessary to take more albedo spectra

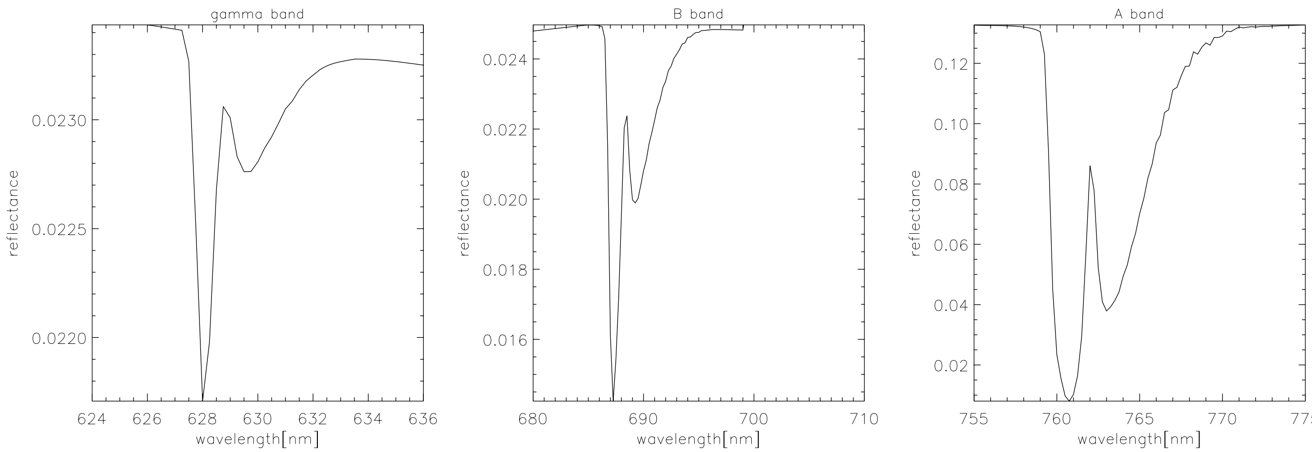

Figure 4:

into account, which will further increase the errors. Additionally, accurate surface albedo spectra for a large number of surface types are hardly available.

4.3 Using Absorption Bands of Oxygen

A third possibility for aerosol retrieval over land is to use measurements of Q in the full spectral range 335-800 nm, combined with intensity measurements in the range 336-384 nm, and additionally intensity measurements in the 3 absorption bands of Oxygen in the GOME-2 spectral range. These Oxygen absorption bands are measured by the main channels of GOME-2 with a spectral resolution of about 0.3-0.4 nm. Figure 4 shows radiative transfer calculations for the 3 Oxygen absorption bands convoluted with the spectral response function of GOME-2.

van Diedenhoven et al. [2005] showed that measurements in the Oxygen-A band allow to simultaneously retrieve the surface albedo and the apparent Oxygen column. These apparent Oxygen column shows large sensitivity to aerosol properties. So, if the total column of Oxygen is known (which is a realistic assumption because surface pressure is accurately known from meteorological models), it may be expected that the surface albedo can be retrieved simultaneously with aerosol properties, using measurements in the Oxygen-A band. A same argumentation holds for the other bands of Oxygen in the GOME-2 spectral range.

To study the use of measurements in the Oxygen absorption bands for aerosol retrievals over land, we used a measurement vector that contains PMD measurements of I in bands 6-8, PMD measurements of Q in bands 6-15, and intensity measurements of the main channels for the spectral ranges of the 3 Oxygen absorption bands (see Fig. 4). For the retrieval we included in the state vector a surface albedo for the range 336-384 nm, a surface albedo for the range 626-636 nm (gamma-band), a surface albedo for the range 680-700 nm (B-band), and a surface albedo for the range 755-775 nm (A-band), in addition to the aerosol parameters.

Figure 5 shows the retrieval error and regularization error on the optical thickness at 550 nm for the corresponding retrievals. Both errors are in the range 0.04-0.06. Thus, the aerosol optical

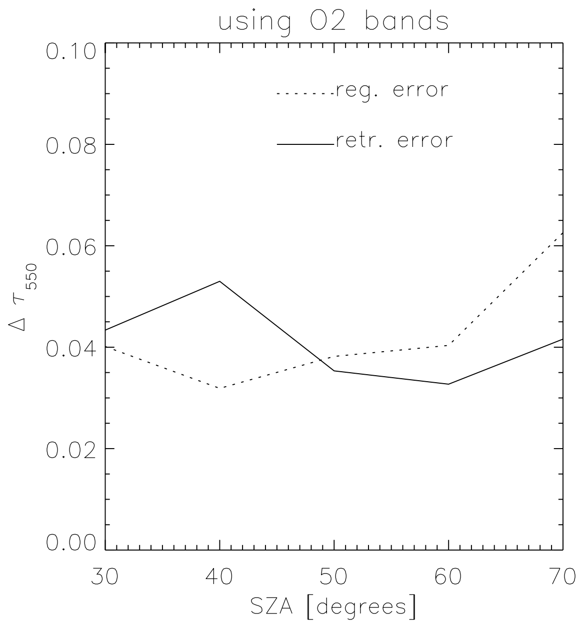

Figure 5: Retrieval error (solid line) and regularization error (dotted line) for retrievals using measurements of I in bands 6-8, PMD measurements of Q in bands 6-15, and intensity measurements of the main channels for the spectral ranges of the 3 Oxygen absorption bands.

thickness is much more accurately retrieved than for the other 2 options discussed above (see Figs. 1 and 3). In fact, the aerosol properties are not affected by the *a priori* values of the surface albedos for these retrievals. So, although the errors on the optical thickness are about a factor 3 higher than for retrievals over the ocean using only PMD measurements [*Hasekamp and Landgraf*, 2005b], this appears to be the best option for aerosol retrieval over land from GOME-2 measurements.

In order to investigate which aerosol parameters are retrieved from the measurement and which parameters are mainly determined by *a priori* information, Fig. 6 shows the derivatives of the retrieved parameters with respect to their *a priori* values. Here, if for a parameter $\partial x/\partial x_a = 1$ this parameter is fully determined by its *a priori* value whereas if $\partial x/\partial x_a = 0$ the parameter is not influenced by its *a priori* value at all. Here, it is important to note that due to our choice of the matrix $\mathbf{\Gamma}$ in (6) we force the aerosol columns of both modes to be fully independent of their *a priori* values, i.e. $\partial x/\partial x_a = 0$ for these parameters. Therefore, these parameters are not included in Fig. 6. It follows from Fig. 6 that the effective radius of the small- and large mode, and both parts of the refractive index can be retrieved with only little influence of *a priori* information. So, important information on aerosol microphysical properties can be retrieved using measurements of Q in the full spectral range 336-800 nm, combined with intensity measurements in the range 336-384 nm, and additionally intensity measurements in the 3 absorption bands of Oxygen.

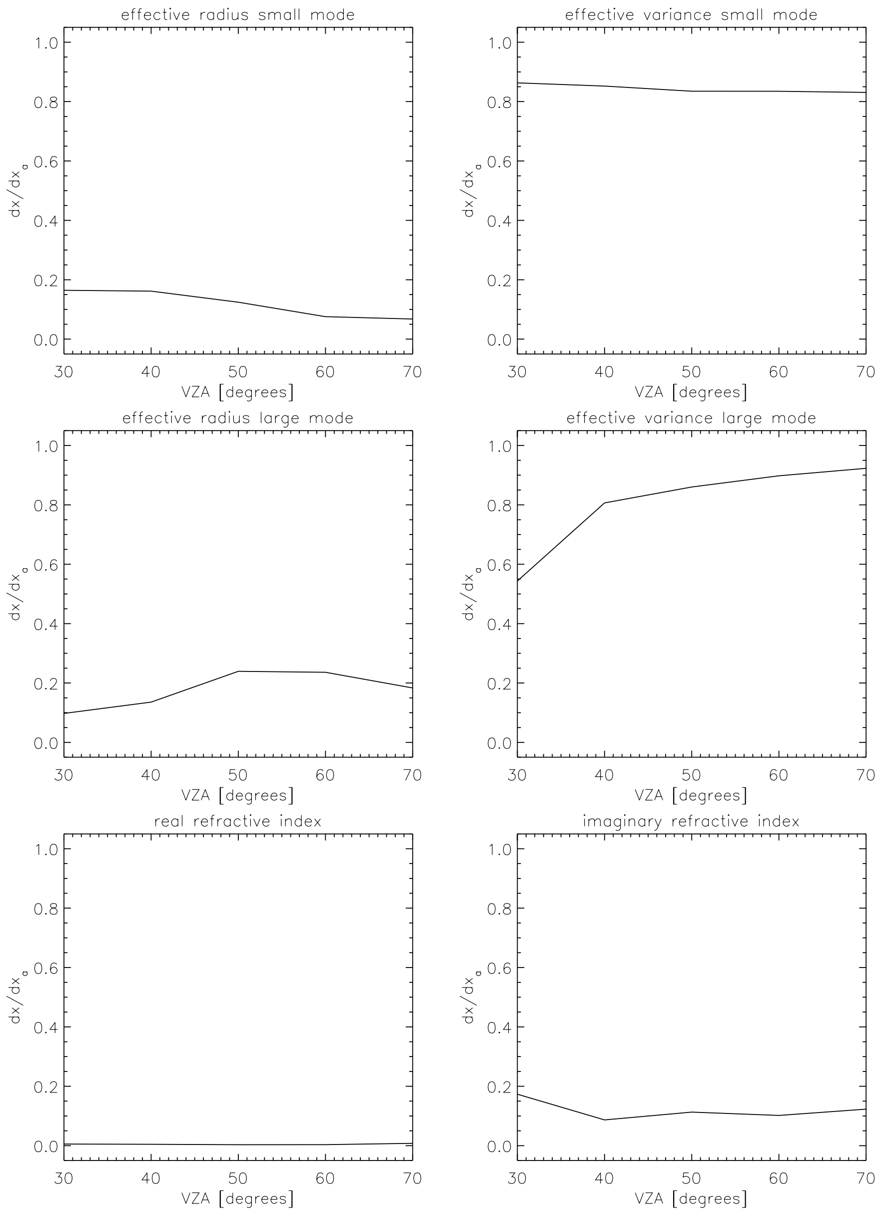

Figure 6: Derivative of retrieved value with respect to *a priori* value for the effective radius of both modes, the effective variance of both modes, and the real- and imaginary- part of the refractive index.

5 Conclusions

In this study, the possibilities for aerosol retrieval over land from GOME-2 measurements were investigated. It was found that if we reduce the measurement vector such that it only contains measurements with small sensitivity to surface reflection (intensity in the spectral range 336-384 nm and Stokes parameter Q in the range 336-800 nm), the retrieved optical thickness depends strongly on *a priori* information on aerosol microphysical properties. This may lead to errors in the optical thickness at 550 nm in the range 0.15-0.25. Similar errors were found for retrievals that use the full spectral range 336-800 nm for both I and Q, but that fit coefficients for 5 standard albedo spectra together with the aerosol parameters. However, errors of the latter retrievals may be expected to increase if more albedo spectra are taken into account. Furthermore, accurate surface albedo spectra for a large number of surface types are hardly available.

The errors are substantially smaller for retrievals that use measurements of Q in the full spectral range 335-800 nm, combined with intensity measurements in the range 336-384 nm, and additionally intensity measurements in the 3 absorption bands of Oxygen. This measurement vectors allows to retrieve a state vector that includes a surface albedo for the range 336-384 nm, a surface albedo for the range 626-636 nm (gamma-band), a surface albedo for the range 680-700 nm (B-band), and a surface albedo for the range 755-775 nm (A-band), in addition to the aerosol parameters. For these retrievals both the retrieval error and regularization error are in the range 0.04-0.06. Furthermore, he effective radius of the small- and large mode, and both parts of the refractive index can be retrieved with only little influence of *a priori* information. A possible drawback of using measurements in the Oxygen absorption bands is that retrievals have to be performed at the spatial resolution of the main channels (40×40 km^2) which is significantly worse than the spatial resolution of the PMD measurements (5×40 km^2). This will result in the availability of less cloud free ground scenes, which is an important requirement for satellite aerosol retrievals.

References

Chowdhary, J., B. Cairns, M. Mishchenko, and L. Travis, Retrieval of aerosol properties over the ocean using multispectral and multiangle photopolarimetric measurements from the Research Scanning Polarimeter, *Geophys. Res. Let.*, *28*, 243–246, 2001.

Chowdhary, J., B. Cairns, and L. Travis, Case studies of aerosol retrieval over the ocean from multiangle, multispectral photopolarimetric remote sensing data, *J. Atmos. Sci.*, *59(3)*, 383–397, 2002.

Chowdhary, J., B. Cairns, M. Mishchenko, P. Hobbs, G. Cota, J. Redemann, K. Rutledge, B. Holben, and E. Russel, Retrieval of aerosol scattering and absorption properties from photopolarimetric observations over the ocean during the clams experiment, *J. Atmos. Sci.*, *62(4)*, 1093–1117, 2005.

Deuzé, J. L., P. Goloub, M. Herman, A. Marchand, G. Perry, S. Susana, and D. Tanré, Estimate of the aerosol properties over the ocean with POLDER, *J. Geophys. Res.*, *105*, 15,329–15,346, 2000.

Deuzé, J. L., et al., Remote sensing of aerosols over land surfaces from POLDER-ADEOS-1 polarized measurements, *J. Geophys. Res.*, *106*, 4913–4926, 2001.

Dubovik, O., B. Holben, T. F. Eck, A. Smirnov, Y. J. Kaufman, M. D. King, D. Tanré, and I. Slutsker, Variability of Absorption and Optical Properties of Key Aerosol Types Observed in Worldwide Locations., *Journal of Atmospheric Sciences*, *59*, 590–608, 2002.

Hansen, J. E., and L. D. Travis, Light scattering in planetary atmospheres, *Space Sci. Rev.*, *16*, 527–610, 1974.

Hansen, P., Analysis of discrete ill posed problems by means of the L-curve, *SIAM Rev.*, *34*, 561–580, 1992.

Hansen, P., and D. O'Leary, The use of the L-curve in the regularization of discrete ill posed problems, *SIAM J. Sci. Comput.*, *14*, 1487–1503, 1993.

Hasekamp, O., and J. Landgraf, A linearized vector radiative transfer model for atmospheric trace gas retrieval, *J. Quant. Spectrosc. Radiat. Transfer*, *75*, 221–238, 2002.

Hasekamp, O., J. Landgraf, W. Hartmann, and I. Aben, Proposal for gome-2 pmd wavelength band selection and the effect on aerosol retrieval, *Techn. Rep. SRON-EOS/RP/04-002*, SRON, Utrecht, the Netherlands, 2004.

Hasekamp, O. P., and J. Landgraf, Linearization of vector radiative transfer with respect to aerosol properties and its use in satellite remote sensing, *Journal of Geophysical Research (Atmospheres)*, *110*, 4203–+, 2005a.

Hasekamp, O. P., and J. Landgraf, Retrieval of aerosol properties over the ocean from multispectral single-viewing-angle measurements of intensity and polarization: Retrieval approach, information content, and sensitivity study, *Journal of Geophysical Research (Atmospheres)*, *110*, 20,207–+, doi:10.1029/2005JD006212, 2005b.

Herman, M., J.-L. Deuzé, A. Marchand, B. Roger, and P. Lallart, Aerosol remote sensing from POLDER/ADEOS over the ocean: Improved retrieval using a nonspherical particle model, *Journal of Geophysical Research (Atmospheres)*, *110*, 10–+, 2005.

Koepke, P., and M. Hess, Scattering functions of tropospheric aerosols: The effect of nonspherical particles, *Appl. Opt.*, *27*, 2422–2430, 1988.

Kokhanovsky, A. A., Optical properties of irregularly shaped particles, *Journal of Physics D Applied Physics*, *36*, 915–923, 2003.

Mishchenko, M., and L. Travis, Light scattering by polydispersions of randomly oriented spheroids with sizes comparable to wavelengths of observation, *Appl. Opt.*, *33*, 7206–7225, 1994.

Mishchenko, M., I. Geogdzhayev, B. Cairns, W. Rossow, and A. Lacis, Aerosol retrievals over the ocean by use of channels 1 and 2 AVHRR data: sensitivity analysis and preliminary results, *Appl. Opt.*, *36*, 7325–7341, 1999.

Mishchenko, M. I., and L. D. Travis, Satellite retrieval of aerosol properties over the ocean using polarization as well as intensity of reflected sunlight, *J. Geophys. Res.*, *102*, 16,989–17,013, 1997a.

Mishchenko, M. I., and L. D. Travis, Satellite retrieval of aerosol properties over the ocean using measurements of reflected sunlight, *J. Geophys. Res.*, *102*, 13,543–13,553, 1997b.

Mishchenko, M. I., A. A. Lacis, B. Carlson, and L. Travis, Nonsphericity of dust-like tropospheric aerosols: Implications for aerosol remote sensing and climate modeling, *Geophys. Res. Lett.*, *22*, 1077–1980, 1995.

Phillips, P., A technique for the numerical solution of certain integral equations of the first kind, *J. Assoc. Comput. Mach.*, *9*, 84–97, 1962.

Rodgers, C., *Inverse methods for Atmospheric Sounding: Theory and Practice*, World Sc.,River Edge, N. J., 2000.

Rodgers, C. D., and B. J. Connor, Intercomparison of remote sounding instruments, *Journal of Geophysical Research (Atmospheres)*, *108*, 13–+, 2003.

Tanré, D., Y. Kaufman, M. Herman, and S. Mattoo, Remote sensing of aerosol properties over the ocean using the MODIS/EOS spectral radiances, *J. Geophys. Res*, *102*, 16,971–16–988, 1999.

Tikhonov, A., On the solution of incorrectly stated problems and a method of regularization, *Dokl. Akad. Nauk SSSR*, *151*, 501–504, 1963.

Torres, O., R. Decae, P. Veefkind, and G. de Leeuw, Omi aerosol retrieval algorithm, *ATBD-OMI-03*, pp. 47–69, 2001.

Torricella, F., E. Cattani, M. Cervoni, R. Guzzi, and C. Levoni, Retrieval of aerosol properties over the ocean using Global Ozone Monitoring Experiment measurements: Method and application to test data, *J. Geophys. Res.*, *104*, 12,085–12,098, 1999.

Travis, L. D., Earth Observing Scanning Polarimeter, in *Long-term monitoring of global climate forcings and feedbacks*, vol. 3234, edited by J. Hansen, W. Rossow, and I. Fung, pp. 40–46, NASA Conf. Publ., 1993.

van de Hulst, H. C., *Light scattering by small particles*, J. Wiley and sons, New York, 1957.

van Diedenhoven, B., O. P. Hasekamp, and I. Aben, Surface pressure retrieval from SCIAMACHY measurements in the O2 A Band: validation of the measurements and sensitivity on aerosols, *Atmospheric Chemistry & Physics*, *5*, 2109–2120, 2005.

Veefkind, J., G. de Leeuw, P. Stammes, and R. Koelemeijer, Regional distribution of aerosols over land derived from ATSR-2 and GOME, *Remote Sens. Env.*, *74*, 377–386, 2000.

Wiscombe, W., and G. Grams, Scattering from nonspherical Chebyshev particles,2, Means of angular scattering patterns., *Appl. Opt.*, *27*, 2405–2421, 1988.